Hardness Controlled Enzymes and Electronegativity Controlled Enzymes: Role of an Absolute Hardness–Electronegativity (η–χ) Activity Diagram as a Coordinate for Biological Activities

Shigeki KOBAYASHI,*[,a] Hajime HAMASHIMA,[b] Masaaki KURIHARA,[c] Naoki MIYATA,[c] and Akira TANAKA*[,a]

Department of Drug Analysis,[a] and Department of Microbiology,[b] Showa College of Pharmaceutical Sciences, 3–3165 Higashi-tamagawagakuen, Machida, Tokyo 194–0042, Japan, and Division of Organic Chemistry,[c] National Institute of Health Science, 1–18–1 Kamiyoga, Setagayaku, Tokyo 158–0098, Japan.
Received September 29, 1997; accepted April 20, 1998

We found that absolute hardness–absolute electronegativity (η–χ) activity diagrams play an important role as a new coordinate of bioactivity in structure-activity relationships. In this paper, the η–χ activity diagram, focusing on the molecular mechanism of bioactive compounds is used to discuss two major problems. First, the potency of bioactivities for xenobiotics such as polychlorinated dibenzo-*p*-dioxins (PCDDs) 3 and polychlorinated biphenyls (PCBs) 4, were found to be strongly related to their absolute hardness (η). Second, the antibacterial activity of new quinolones such as norfloxacin 1 and enoxacin 2, was found to be strongly related to their absolute electronegativity (χ). These findings predict at least two chemical properties for a hardness-controlled or electronegativity-controlled enzyme.

Key words hardness concept; η–χ activity diagram; biological activity; new quinolone; dioxin; PCB

One of the major goals of structure–activity relationships (SARs) for the design of drugs in medicinal chemistry and pharmacology is understanding of the molecular mechanism for a drug–enzyme complex in living systems. Many useful and important quantum mechanical methods have been widely used for SARs studies.[1] The nature of the interaction of substrate with enzyme and receptor also can be investigated by more rigorous quantum mechanical methods. In a recent study, we reported that an important relationship between absolute hardness and biological activity exists for environmmental pollutants such as dioxins **3**,[2] and found that absolute hardness–absolute electronegativity (η–χ) activity diagrams play an important role as a new coordinate of bioactivity in the study of SARs.[3]

In this study, η–χ activity diagrams, focusing on the molecular mechanism of the bioactive compounds, are used to investigate two major problems. First, the potency of bioactivities of xenobiotics, such as polychlorinated dibenzo-*p*-dioxins (PCDDs) **3** and polychlorinated biphenyls (PCBs) **4**[4] (Chart 1), was determined to be strongly related to the values of their absolute hardness (η). Second, the potency of activities for new quinolones, such as norfloxacin **1b** and enoxacin **2b** (Chart 1),[5] which are active against gram-negative and -positive bacteria, were examined and determined to be related to the values of their absolute electronegativity (χ). This indicates that some biological activities and/or toxicities are controlled by absolute hardness or electronegativity, suggesting that the corresponding target enzymes (or receptors) can also be classified as hardness or electronegativity controlled types. The findings in the present study predict at least two chemical properties for hardness-controlled and electronegativity-controlled enzymes.

According to the hardness concept,[6] a hardness controlled acid (or base) prefers to interact with a hardness controlled base (or acid), and an electronegativity controlled acid (or base) prefers to interact with an electronegativity controlled base (or acid). Therefore, the chemical characteristics of drugs (or chemicals) based on absolute hardness or absolute electronegativity are an extremely useful tool for drug design, toxicity prediction, and analysis of mechanisms of bioactive compounds.

Experimental

We employed semiempirical PM3 and AM1 calculations in the SPARTAN programs[7] to determine the electronic structure of optimized chemicals. The hardness concept has been applied to many problems in organic chemistry.[6] Recently, we used the concept to elucidate the relationship between chlorination pattern and toxicity or induction responses in dioxins.[3] The values of absolute hardness and absolute electronegativity were provided by density functional theory in chemical systems.[8]

$$\chi = -\mu = (\partial E/\partial N)_v \quad (1)$$

$$\eta = 1/2(\partial^2 E/\partial N^2)_v \quad (2)$$

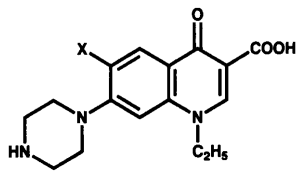

1

1a: X=F 1e: X=H
1b: X=Cl 1f: X=NO2
1c: X=Br 1g: X=OH
1d: X=I 1h: X=NH2

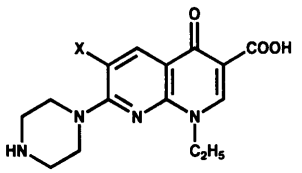

2

2a: X=F 2e: X=H
2b: X=Cl 2f: X=CN
2c: X=Br 2g: X=OH
2d: X=I 2h: X=NH2

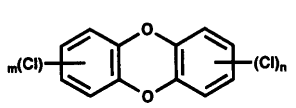

3

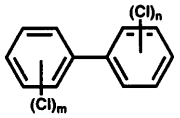

4

Chart 1. Structures of Quinolines **1**, 1,8-Naphthyridines **2**, Dibenzo-*p*-dioxins **3**, and Biphenyls **4**

* To whom correspondence should be addressed.

where μ is the chemical potential, E is the electronic energy, N is the number of electrons, η is the absolute hardness, and χ is the absolute electronegativity, respectively. In this hardness concept, electronegativity changes the electron density around a molecule, and the hardness is a measure of the resistance to change in electron density. The η is a half value of the energy gap between HOMO (highest occupied molecular orbital) and LUMO (lowest unoccupied molecular orbital), and χ is a half value of their energy sum. The most notable chemical consequence of the hardness concept is that a soft molecule interacts with a soft molecule, and a hard molecule with a hard molecule.

DNA Topoisomerase and Ah Receptor Quinolone antibacterials are known to be highly specific inhibitors of DNA gyrase(bacterial DNA topoisomerase II). The process of inhibition of DNA gyrase, expressed as IC_{50} (μg, ml) has been suggested to be reversible binding of the quinolone, for example norfloxacin, with the bacterial DNA topoisomerase.[9] Quinolones have been shown to bind specifically to a binding site in the α subunit of the bacterial topoisomerase DNA gyrase(type II DNA topoisomerase), and that inhibition of DNA gyrase leads to the death of bacterial cells.[9]

Biological responses of xenobiotics such as PCDDs, PCBs, and polychlorinated dibenzofurans (PCDFs), *etc.* are considered to be mediated through an intracellular cytosolic receptor, the arylhydrocarbon receptor(AhR). The toxicity and induction responses have been proposed to involve the initial non-covalent binding of these congeners to the AhR in the cytosol which is encoded by the Ah gene.[4,10] This receptor from C57BL/6J mice consists of 805 amino acids, and has a molecular weight of about 90 kD.[11] Its primary characteristics are the result of the abundancy of aromatic and hydrophobic amino acids in its sequence; aromatic amino acids comprise 8.4% of the total.

According to the hardness concept, soft acids in a chemical system will prefer to coordinate to soft bases, and hard acids will prefer hard bases. If the chemical property of a dioxin is more soft than an other, biological activity is more potent. However, the chemical properties of DNA gyrase are determined by the absolute electronegativity, as shown in Results.

Results

Antibacterial Activity of New Quinolones Potent antibacterial drugs such as norfloxacin **1b** and enoxacin **2b**, have a basic pyridonecarboxylic acid skeleton, of all of which possess a 1,4-dihydro-4-oxopyridine-3-carboxylic acid moiety. Introduction of -F or -Cl at C-6 strikingly influenced the antibacterial activities. What is the significance of the C-6-fluoro group? This important effect has been considered by many medicinal chemists, however fundamental understanding is still lacking.

We applied the hardness concept method to attempt to elucidate the relationship between chemical structure and activity(MICs) for the antibacterial quinolones. Table 1 shows the *in vitro* antibacterial activity of drugs **1** and **2** derivatives, cited from the literature,[12] against representative gram-positive (*Staphylococcus aureus* 209P JC-1) and gram-negative bacteria (*Escherichia coli* NIHJ JC-2). In the series of drugs represented by **1**, activity against *E. coli* NIHJ JC-2 increases in the order $-OH < -NH_2 < -H < -Br < -Cl < -F$. In the series of drugs represented by **2**, activity against the same bacteria increases in the order $-OH < -I < -H < -NH_2 < -Br < -CN < -Cl < -F$. Specifically, substitution of –F or –Cl at the C-6 position causes a marked increase in activity. We thus proposed our new

Table 1. *In Vitro* Antibacterial Activity (MIC), DNA Gyrase Activity (IC_{50}) and Calculated η and χ Values for 4-Oxo-3-quinolinecarboxylic Acid Derivatives

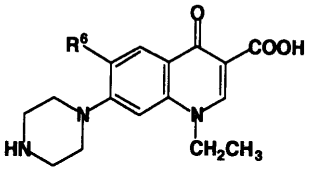

No.	R^6	η (eV)[a]	χ (eV)[a]	DNA gyrase activity (mM)[b]	MIC (mM)[c]
1a	F	4.005	5.115	2.006×10^{-3}	1.567×10^{-4}
1b	Cl	3.993	5.047	2.624×10^{-3}	2.980×10^{-4}
1c	Br	4.034	5.022	9.421×10^{-3}	20.53×10^{-4}
1d	I	3.963	4.934	—	—
1e	H	4.073	4.968	15.32×10^{-3}	25.91×10^{-4}
1f	NO_2	4.023	5.571	14.83×10^{-3}	22.54×10^{-4}
1g	OH	3.935	4.918	25.52×10^{-3}	394.3×10^{-4}
1h	NH_2	3.860	4.738	51.58×10^{-3}	99.00×10^{-4}

a) PM3 level. *b*) IC_{50}, taken from ref. 5*b*. *c*) *E.coli* NIHJ JC-2, taken from ref. 5*b*.

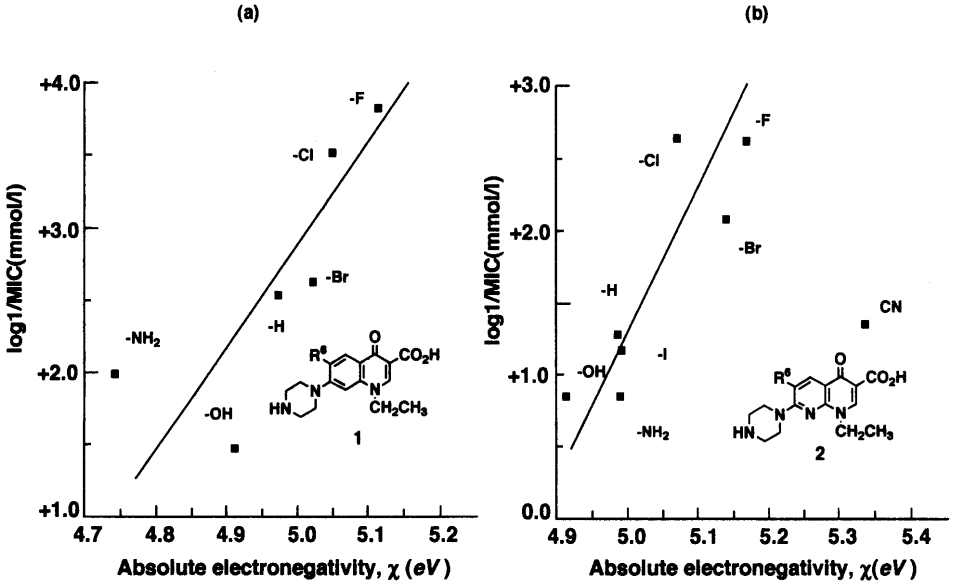

Fig. 1. Plots of MIC (mmol) against *E. coli* NIHJ JC2 *vs.* Calculated Absolute Electronegativity (χ) for the 1,4-Dihydro-4-oxo-1,8-naphthyridine-3-carboxylic Acid Antibacterials (a) and 1,4-Dihydro-4-oxo-3-quinolinecarboxylic Acid Antibacterials (b)

MIC data were taken from ref. 5.

Table 2. *In Vitro* Antibacterial Activity (MIC) and Calculated η and χ Values of 4-Oxo-1,8-naphthyridine-3-carboxylic Acid Derivatives

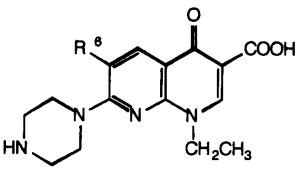

No.	R^6	η (eV)[a]	χ (eV)[a]	MIC (mM)[b]	MIC (mM)[c]
2a	F	3.947	5.159	3.125×10^{-4}	2.445×10^{-3}
2b	Cl	3.924	5.063	23.14×10^{-4}	2.320×10^{-3}
2c	Br	3.981	5.138	40.94×10^{-4}	8.236×10^{-3}
2d	I	3.901	4.984	584.1×10^{-4}	58.55×10^{-3}
2e	H	4.029	4.973	206.9×10^{-4}	41.53×10^{-3}
2f	CN	3.916	5.345	23.85×10^{-4}	38.34×10^{-3}
2g	OH	3.867	4.905	3144×10^{-4}	157.7×10^{-3}
2h	NH_2	3.850	4.982	197.0×10^{-4}	19.78×10^{-3}

a) PM3 level. *b*) *E. Coli* NIHJ JC-2, taken from ref. 12*a*. *c*) *S. aureus* 209PJC-1, taken from ref. 12*a*.

idea in order to solve the relationship between activity and structure in series **1** and **2**.

Figures 1a and 1b shows a plot of absolute electronegativity *vs.* MIC ($\log 1/M$) for norfloxacin and enoxacin analogs, respectively. All values of χ and η, were obtained from Eqs. 1 and 2, respectively, and are summarized in Tables 1 and 2. Good linear correlation indicates the dependence of antibacterial activity (MIC, mmol/l) against *E. coli* NIHJ JC-2 on absolute electronegativity for derivatives **1**. Enoxacin derivatives **2** also displayed a linear correlation between MIC ($\log 1/M$) and absolute electronegativity, as shown in Fig. 1b. These linear correlations are completely dependent on the magnitude of the absolute electronegativity value.

The substitution effect of F- at C-6 is clearly seen in comparison with that of I- and HO- on the 4-oxo-3-quinoline parent skeleton. For instance, χ-value of the F–derivative **1a** is the largest value ($\chi=5.12$) (except for $-NO_2$). Although the η-value for H- at C-6 is large ($\eta=4.07$), no antibacterial activity is observed. With regards to quinolone SARs, we depicted the η–χ activity diagrams of η and χ as coordinates of the biological activity of **1** and **2**, as shown in Figs. 2 and 3. We used absolute electronegativity as the abscissa and absolute hardness as the ordinate. Our findings imply that antibacterial activities are controlled by absolute electronegativity but not by absolute hardness. Therefore, we concluded that the antibacterial activity of new quinolones (*e.g.* **1a**: norfloxacin and **2a**: enoxacin) substituted at the C-6 position show a satisfactory correlation with absolute electronegativity (χ).

Anti-DNA Topoisomerase II Activity of New Quinolones In order to understand the effect of the C-6 substituents on DNA gyrase inhibiton, we compared DNA gyrase inhibition activities with absolute hardness (and absolute electronegativity) for **1**. The 50% inhibition activity of DNA gyrase assesed as the relaxed⇄supercoiled DNA transformation,[13] and values of χ and η for the groups, are given in Table 1. From the plot as a function of absolute electronegativity (Fig.4), increase in inhibition activity is

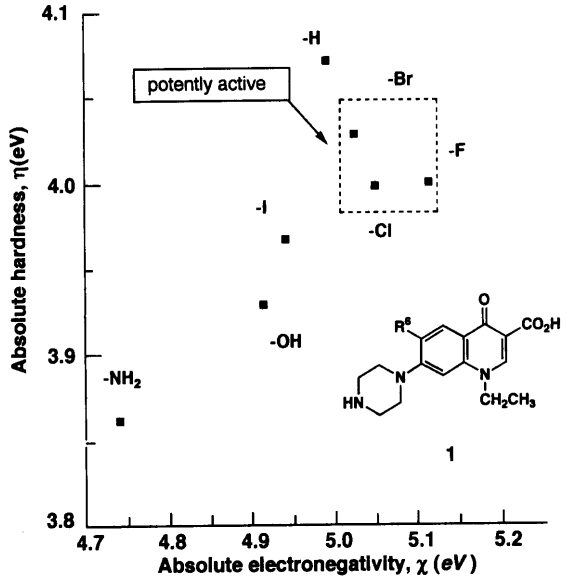

Fig. 2. Plot of Absolute Hardness–Electronegativity Activity Diagram for Quinoline Antibacterials

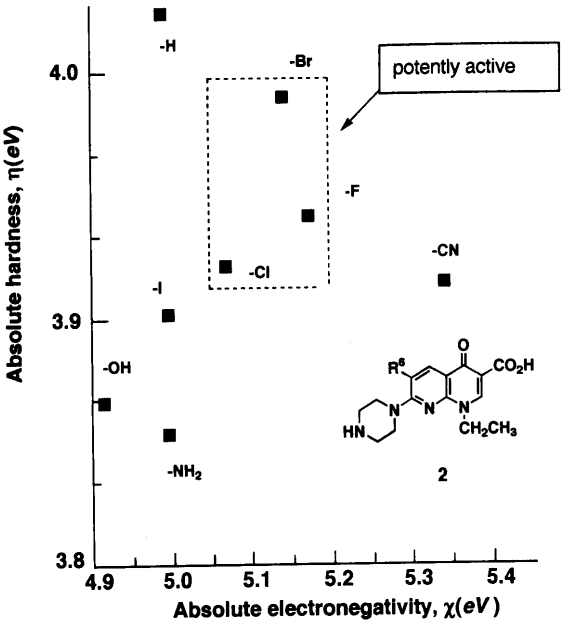

Fig. 3. Plot of Absolute Hardness–Electronegativity Activity Diagram against 1,8-Naphthyridine Antibacterials

proportional to increasing absolute electronegativity in the order, $-NH_2<-NO_2<-H<-OH<-Br<-Cl<-F$. The inhibition activity of DNA gyrase is not always correlated with the steric hindrance of the substituents groups, but is preferably dependent on the values of χ. As expected, higher inhibition occurs with the larger χ value, and this is equal to the order for antibacterial activity.

For these results, the substituent effect at the C-6 position of norfloxacin also plays an important role in the inhibition of DNA gyrase. Obviously, since absolute electronegativity indicates the change in electron density around the molecule and atom, the value of electronegativity increases by introduction of fluorine and chlorine at C-6 position of **1** and **2**, as shown in Chart 2. This increase indicates that hydrogen bonding and charge transfer should be essential chemical interactions for the

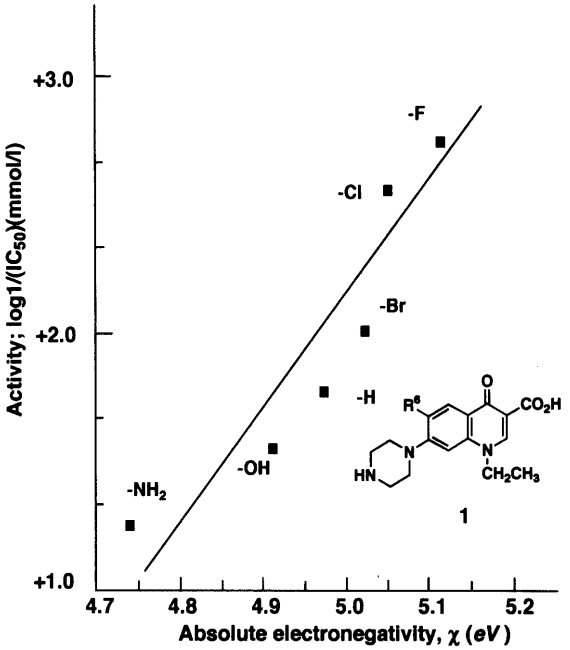

Fig. 4. Plot of IC_{50} (mmol) against Antibacterial DNA Topoisomerse II Activity *vs.* Calculated Absolute Electronegativity (χ) for 1,4-Dihydro-4-oxo-3-quinoline-carboxylic Acid Antibacterials

IC_{50} data were taken from ref. 9*a*.

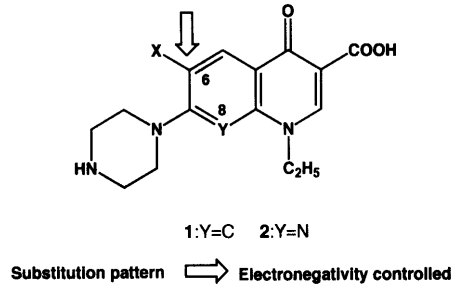

Chart 2

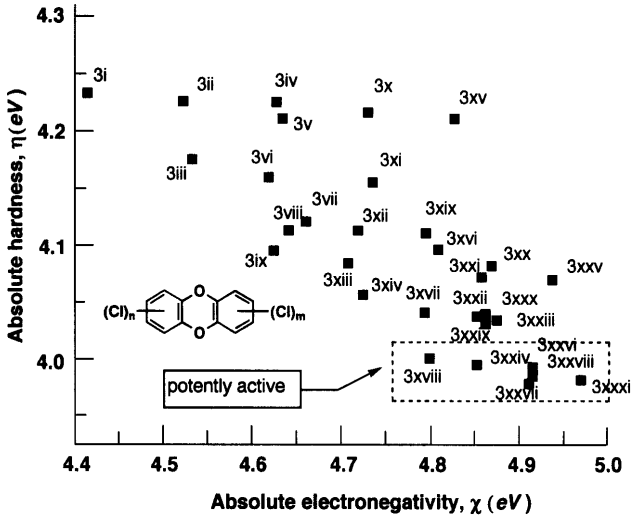

Fig. 5. Plot of Absolute Hardness–Electronegativity Activity Diagram against Polychlorinated Dibenzo-*p*-dioxins

Highly toxic dioxins are distributed in the dashed circle. **3i**, DD; **3ii**, 1-; **3iii**, 2-; **3iv**, 1,6-; **3v**, 1,4-; **3vi**, 1,2-; **3vii**, 2,7-; **3viii**, 2,8-; **3ix**, 2,3-; **3x**, 1,4,6-; **3xi**, 1,6,8-; **3xii**, 1,2,7-; **3xiii**, 1,2,3-; **3xiv**, 2,3,7-; **3xv**, 1,4, 6,9-; **3xvi**, 1,2,6,8-; **3xvii**, 1,2,3,7-; **3xviii**, 2,3,7,8-; **3xix**, 1,2,6,7-; **3xx**, 1,2,3,6,9-; **3xxi**, 1,2,3,4,9-; **3xxii**, 1, 2,3,6,7-; **3xxiii**, 1,2,3,6,8-; **3xxiv**, 1,2,3,7,8-; **3xxv**, 1,2, 3,4,6,9-; **3xxvi**, 1,2,3,6,7,8-; **3xxvii**, 1,2,3,7,8,9-; **3xxviii**, 1,2,3,4,7,8-; **3xxix**, 1,2,3,4,7,-; **3xxx**, 1,2,4,7,8-; **3xxxi**, 1,2,3,4,6,7,8-.

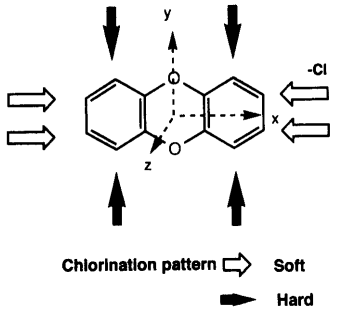

Chart 3

antibacterial drug, norfloxacin. This striking effect shows that C-6 substitution of norfloxacin controls the magnitude of the χ value.

Dioxins Polyhalogenated aromatic hydrocarbons such as PCDDs (**3**) and PCBs (**4**), having varying chemical structures, as shown in Chart 1, are highly toxic environmental pollutants with potent induction responses and toxic potency. Especially, 2,3,7,8-tetrachlorinated dibenzo-*p*-dioxin (2,3,7,8-TCDD), one of the most potent artificial toxic chemicals, is a well-known prototype.[4] The toxicity and induction responses of these classes are dependent on their chlorine substitution pattern, the number, and the position of the chlorinated congeners. Lateral substitution is particularly important.

The toxicity and induction responses of dioxins also display a good linear correlation with their absolute hardness, provided by the hardness concept. We have shown that the correlation curve obtained by plotting the η value of dioxins against the logarithm of their ability to induce arylhydrocarbon hydroxylase (AHH) and ethoxy resorufin O-deethylase (EROD) activity, is related to thymic atrophy *in vivo*, and acute toxic activity.[2a,3] This figure implies that the induction ability of dioxins is in good proportion to the η value. In Fig. 5, the value of η as the coordinate of biological activity is given as a function of absolute electronegativity for the 30 dioxins. As a result, the most toxic dioxins are distributed within the dotted line in the circle, and have a small η value. The soft dioxins have more potent biological activity than the hard dioxins. If the number of chlorine substituents is equal, chlorination at the lateral positions on the dibenzo-*p*-dioxin (DD) skeleton is more soft than that at the other positions, as shown in Chart 3. Thus, we suggest that the η–χ activity diagram is able to predict the strength of toxicity for new types of toxic chemicals.

PCBs The numerous induction response properties of PCBs **4** can be classified into two types: phenobarbital (PB-) type and 3-methylcholanthrene (MC-) type,[14,15] which have the ability to induce hepatic microsomal cytochrome P-450 and P-448 (mono-oxygenase) activities, respectively. Moreover, the mechanisms for these two types remain to be clarified. It has been reported that chlorination at both *para*- and, at least, two *meta*-positions resulted in maximum activity, whereas at the *ortho*-position resulted in decreased activity. The potency of cytochrome P-450 induction decreases in the following order: 3,4,5,3′,4′,5′-PCB > 3,4,5,3′,4′-PCB > 2,3,4,3′,4′-

Table 3. Calculated Values of η and χ for Polychlorinated Biphenyls

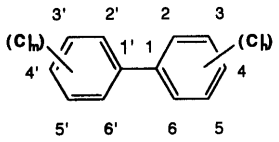

Chlorination	Absolute hardness η (eV)[a]	Absolute electronegativity χ (eV)[a]	Torsional angle[b] ϕ	Chlorination	Absolute hardness η (eV)[a]	Absolute electronegativity χ (eV)[a]	Torsional angle[b] ϕ
2,4,6,2',4',6'-	4.370	5.063	74	3,4,3',4'-	4.183	4.931	49
2,4,5,2',4',5'-	4.191	4.999	67	3,4,5,3',4'-	4.154	5.012	49
2,3,4,2',3',4'-	4.276	5.027	67	3,4,5,3',4',5'-	4.130	5.087	49
2,3,6,2',3',6'-	4.316	4.914	74	2,3,4,3',4'-	4.242	4.973	62
3,4,2',4'-	4.267	4.910	62	Non	4.460	4.640	42
2,5,2',5'-	4.377	4.845	67				

a) PM3 level. *b*) Taken from ref. 16.

PCB > 3,4,3',4'-PCB > 2,4,3',4'-PCB > 2,5,2',5'-PCB.[15] Further, the potency of benzo[*a*]pyrene 3-hydroxylation activity also decreases in the same order.[15] Obviously, a pattern exists in the relation between induction activity (and toxicity) and chlorination.

Since PCBs have a non-planar conformation due to steric repulsion between the phenyl rings, the experimental torsional angle (ϕ), which has been previously measured by photoelectron spectroscopic (PES) studies was used to determine the electronic structure of optimized PCBs.[16] The results of the absolute hardness (η) and absolute electronegativity (χ), as determined by PM3 calculations, are summarized in Table 3. The difference in the η value of 3,4,5,3',4',5'-PCB (η=4.13) and 2,3,4,2',3',4'-PCB (η=4.28) shows a typical trend in the effect of chlorine substitution between the *ortho*-position, and the *para*- and *meta*-positions on the biphenyl skeleton. Planar type PCBs have lower η values than of non-planar types. The η values are strongly affected by the chlorination pattern. That is, planar PCBs are soft and non-planar PCBs are hard.

Figures 6a and b show the correlation curves obtained by plotting η values *vs.* the log of relative benzo[*a*]pyrene activity[15c] and log of relative cytochrome P-450 activity[15c], respectively. Benzo[*a*]pyrene activity and cytochrome P-450 activity of PCBs are found to be proportional to their absolute hardness. Good linear relationships were also observed between absolute hardness and relative DT-diaphorase activity in rats[15c] and relative liver concentration in chicks,[15c] as shown in Figs. 7a and b. These findings show that: (i) soft PCBs have small η values, and potent induction ability, and (ii) the measured η value predicts the toxic potency and induction ability. Nevertheless, the measure χ value does not predict the biological activity for PCBs.

We could successfully classify the type of enzyme induction for PCBs by a η–χ activity diagram. Figure 8 shows a η–χ activity diagram as coordinates of toxicity and induction responses for PCBs. The more toxic, 3,4,5,3',4',5'-PCBs, 3,4,5,3',4'-PCBs, and 3,4,3',4'-PCBs, are distributed within the encircled area (MC-type PCBs) in the figure. The other compounds, with *ortho*-chlorine substituents such as 2,3,4,2',3',4'-PCBs, 2,3,6,2',3',6'-PCBs, and 2,4,6,2',4',6'-PCBs are distributed within the encircled

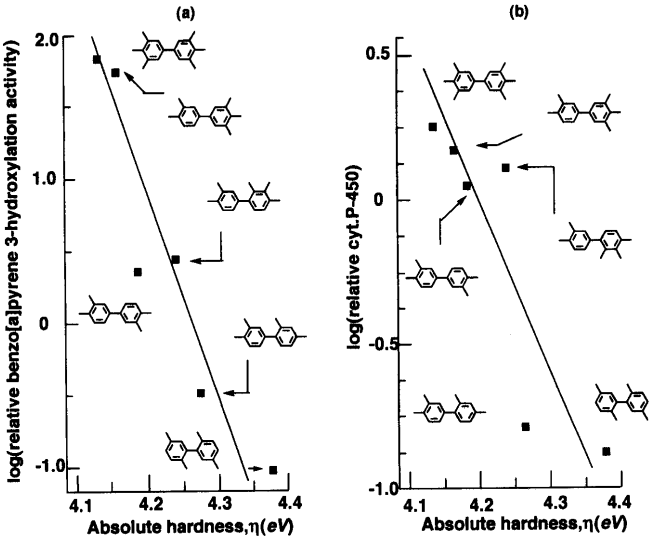

Fig. 6. Correlation Diagram between Absolute Hardness (η) and log(Relative Benzo[*a*]pyrene 3-Hydroxylation Activity) (a) and log (Relative cyt. P-450)(b), Respectively, for PCBs

area of PB-type induction. Planar-type PCBs, such as 3,4,5,3',4'-PCB and 3,4,5,3',4',5'-HCB are known as more toxic than 2,5,2',5'-TCB and 2,4,5,2',4',5'-HCB, *etc.* Our results show that the absolute hardness of MC-type PCBs is smaller than that of PB-type PCBs. The chlorine substituted PCBs at the C-3 and -5 (C-3' and 5') and C-4 (C-4') positions are more soft than those of substituted at C-2 and 6 (C-2' and 6'), as shown in Chart 4.

Discussion

Efforts to predict the biological properties of chemicals is one of the most exciting aspects of life science. At present, however, it is difficult to predict bioactivity and toxicity from the chemical structure. In this work we have attempted to apply the hardness concept to biological activity in order to predict the potency of toxicity, induction ability, bacterial DNA topoisomerase activity, and the antibacterial activity of several drugs. The results show that absolute hardness and electronegativity play a dominant role as a measure of biological activities. Although the biological activities of the highly toxic,

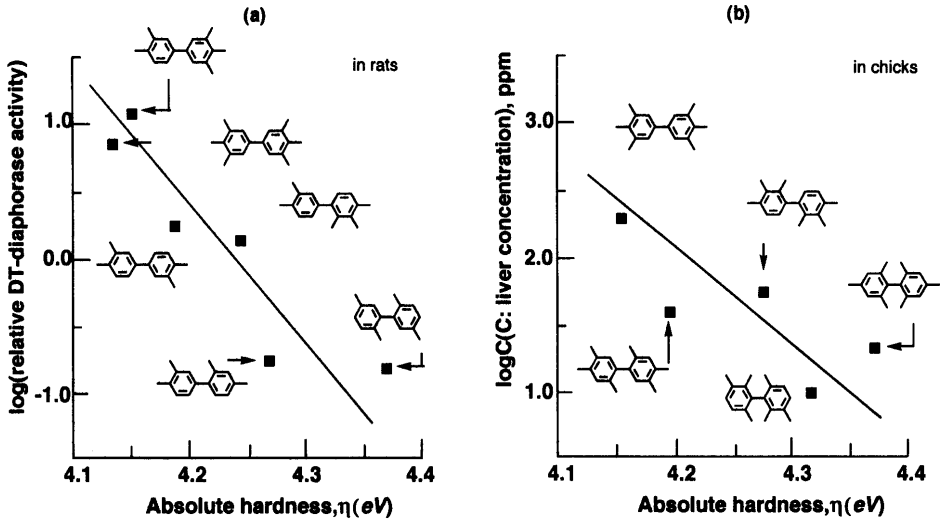

Fig. 7. Correlation Diagram between Absolute Hardness (η) and log(Relative DT-Diaphorase Activity) (a) and log (C: Liver Concentration) (b), Respectively, for PCBs

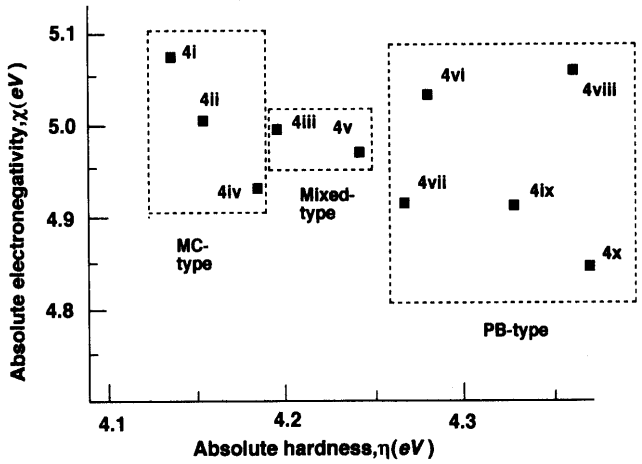

Fig. 8. Plot of Absolute Hardness–Electronegativity Activity Diagram against PCBs

The induction types, MC-type, PB-type, and Mixed-type, for PCBs are classified by this method. **4i**, 3,4,5,3′,4′,5′-; **4ii**, 3,4,5,3′,4′-; **4iii**, 2,4,5,2′,4′,5′-; **4iv**, 3,4,3′,4′-; **4v**, 2,3,4,3′,4′-; **4vi**, 2,3,4,2′,3′,4′-; **4vii**, 3,4,2′,4′-; **4viii**, 2,4,6,2′,4′,6′; **4ix**, 2,3,6,2′,3′,6′-; **4x**, 2,5,2′,5′-.

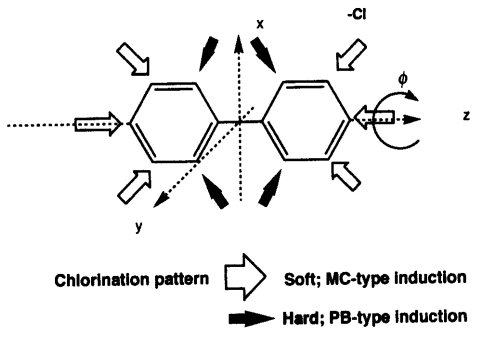

Chart 4

dioxins and PCBs, are controlled by absolute hardness (η), the potencies of MICs and DNA topoisomerase inhibition for therapeutically important antibacterial drugs, *e.g.* norfloxacin and enoxacin, are controlled by absolute electronegativity (χ).

According to the hardness concept, this means that soft molecules (*e.g.* 2,3,7,8-TCDD, 3,4,5,3′,4′-PCB, *etc.*) prefer a soft receptor (*e.g.* Ah receptor) to a hard receptor, and that the electronegativity controlled molecules (*e.g.* new quinolones) prefer an electronegativity controlled receptor (*e.g.* DNA topoisomerase). In the receptor the hardness or electronegativity implies a chemical interaction between the ligand binding site and drug in the receptor. That is, in cells a model for interaction of dioxins (and PCBs) with the Ah receptor is represented by the eqilibrium in Eq. 3, where [ ] is a molecular complex.

$$\text{dioxin} + \text{AhR} \rightleftarrows [\text{dioxin AhR}] \rightarrow \text{move into nucleus} \quad (3)$$

Recently, Burbach *et al.* found that the region, $-^{232}$Asn–^{233}Phe–^{234}Gln–^{235}Gly–^{236}Arg–, lies near the dioxin binding site of the Ah receptor.[11] The residues 243—247 and 278—282 in the Ah receptor which lie near the –Asn–Phe–Gln–Gly–Arg region, contain a $-CONH_2$ group, for example –Asn–Phe– and –Gln–Asn–residues.

Dioxins have oxygens that can potentially form hydrogen bonds with the binding site of AhR. The oxygens (*e.g.* 2,3,7,8-TCDD) easily form hydrogen bonds with the amide proton of Asn and Gln residues. Here, we propose a binding model such as a [–Asn–Phe–Gln($CONH_2\cdots$ Dioxin)–Gly–Arg–] complex and a [–Asn($CONH_2\cdots$ Dioxin)–Phe–Gln–Gly–Arg–] complex.[17] Figure 9 shows the η–χ activity diagram for the model of the drug–Ah receptor complex of 2,3,7,8-TCDD (and 1,4,6,9-TCDD)–(–Asn–Phe –Gln–Gly–Arg–). Although a detailed investigation of the binding site interacting with the dioxin of Ah receptor has not been presented yet, our dioxin–Ah receptor binding model presents a possible view to elucidate SARs and the mechanism of the dioxins. In addition, Fig. 9 indicates that the toxic potency of dioxins correlates with the binding affinity of dioxins to the Ah receptor. It is found that 2,3,7,8-TCDD–Gln complex chlorinated at the 2,3,7,8-positions is chemically most soft and 1,4,6,9-TCDD–Gln complex chlorinated at the 1,4,6,9-positions is most hard, based on the η–χ activity diagram. This means that binding with Gln in the receptor seems to satisfactorily correlate with toxic potency. The absolute hardness produces an effect on the bioactivity of dioxins. This finding shows that absolute hardness is most

important factor, rather than absolute electronegativity in the toxicity of dioxins (and PCBs).

The incorporation of a C-6 fluorine atom to 4-quinolones and 1,8-naphthyridines leads to higher absolute electronegativity, and to remarkably lower hardness. According to the absolute electronegativity, the hydrophobicity of the naphthyridine analoges **1** and **2** play little or no role in antibacterial activity. This result means that the chemical property of C-6 fluorine includes not only ionic binding and nucleophilic attack but also charge transfer. From our proposed model, the anti-bacterial DNA topo II is an electronegativity controlled enzyme since the effectiveness of absolute electronegativity is in proportion to the order of inhibition for bacterial DNA topo II, as shown in Fig. 4. Therefore, it is indicated that direct interaction would occur between norfloxacin and the DNA–DNA topo II complex.[18] The relationship between the χ value and inhibition of DNA topo II is linear, along with inhibition of supercoiled DNA to relaxed DNA by topo II, based on the norfloxacin–topo II binding interaction. Therefore, we propose a model of a chemical equilibrium between DNA, Topo II, and norfloxacin, as shown in Eq. 4.

$$\text{DNA} + \text{TopoII} \rightleftarrows [\text{DNA-TopoII}] \overset{\text{norfloxacin}}{\Longleftrightarrow} [\text{norfloxacin-Topo II-DNA}] \quad (4)$$

The η–χ activity diagram reveals that DNA topo II inhibition of naphthyridine analoges **1** is dependent on the absolute electronegativity, and the fluoro group at C-6 position plays a dominant role in the increase in value of χ. This increase results in a striking increase of bacterial growth inhibition.

Thus, it appears that bacterial DNA topoisomerse II is an absolute electronegativity controlled enzyme and the Ah receptor is an absolute hardness controlled enzyme. This finding shows that enzymes (or receptors) may be classified into at least two types by hardness and electronegativity. Chemicals (or drugs) can similarly be classified into two classes. As summarized in Chart 5, we can predict the magnitude of toxicity and biological activity, based on the chemical properties of PCDDs and norfloxacin, *etc.* The class of electronegativity-controlled chemicals is an interesting group of bioactive compounds. The class of hardness-controlled chemicals displays high toxicity. For example, dichlorodiphenyltrichloro ethane (DDT) analogs are classified as the environmental estrogens,[19] and probably bind with the target enzyme based on a hardness controlled mechanism, since we found that their biological activity is controlled by absolute hardness.[20] Moreover, we can predict that the toxicity of PCDFs is also controlled by absolute hardness. In fact, chemically more soft PCDFs are toxic and active in potency.[2b] The η–χ activity diagrams play a dominant role in the toxicity prediction of chemicals and the development of molecular design.

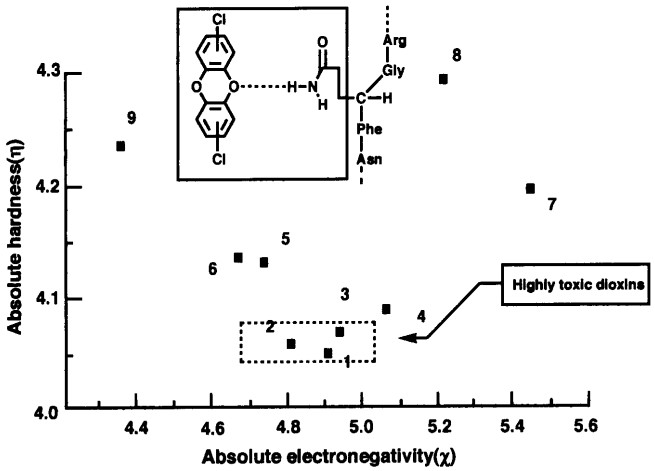

Fig. 9. Absolute Hardness–Absolute Electronegativity Diagram for Glutamine–Dioxin Complexes

More toxic dioxins are distributed within the brokened rectangle. **1**, 2,3,7,8-TCDD; **2**, 1,2,3,7,8-PCDD; **3**, 1,2,3,7,8,9-HCDD; **4**, 2,3,7-TriCDD; **5**, 1,4,6,8-TCDD; **6**, 2,7,-DCDD; **7**, 1,2,4,6,7,9-HCDD; **8**, 1,4,6,9-TCDD; **9**, DD.

Conclusions

In conclusion, the hardness concept indicates that the action of drugs on enzymes (or receptors) is controlled by absolute hardness or absolute electronegativity. By knowing chemical properties of a drug based on the hardness concept, differentiation of absolute hardness controlled or electronegativity controlled enzymes may be possible. As one of the above methods, we found that the η–χ activity diagram is very useful for this differentiation. Moreover, the diagram suggests the chemical mechanism of the drugs on the enzyme. The calculation results clearly demonstrate the biological activities of drugs. For instance, the bacterial DNA topoisomerase II is an absolute electronegativity controlled enzyme and the Ah receptor is an absolute hardness controlled enzyme. Therefore, enzymes(or receptors) can be classified into at least two types.

References and Notes

1) *a*) Hansch C., *Acc. Chem. Res.*, **26**, 147—153 (1993); *b*) Wagener M., Sadowski J., Gasteiger J., *J. Am.Chem. Soc.*, **117**, 7769—7775 (1995); *c*)The concept of hard and soft acids and bases (HSAB) in chemistry was applied to organic chemistry in 1967 by Pearson;

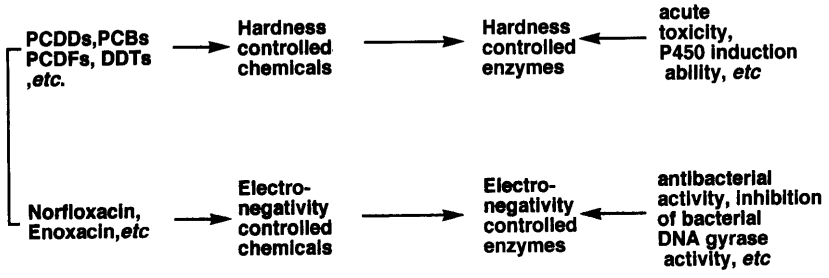

Chart 5. Classification of Bioactivity Using Hardness and Electronegativity of Chemicals

Peason R. G., Songstand J., *J. Am. Chem. Soc.*, **89**, 1827—1836 (1967); *d*) Alonso J. A., Baekelandt B. G., Balbas L. C., Chattaraji P. K., Gazquez J. L., Grice M. E., Komorowski L., March N. H., Mortier W., J., Murray J. S., Nalewajiski R. F., Parr R. G., Pearson R. G., Politzer P.,Schoonheydt R. A., Sen K. D., "Structure and Bonding," Vol. 80, Springer-Verlag, Berlin, Heidelberg, 1993.

2) *a*) Kobayashi S., Saito A., Ishii Y., Tanaka A., Tobinaga S., *Chem. Pharm. Bull.*, **39**, 2100—2105 (1991); *b*) Kobayashi S., Shigihara A., Ichikawa H., Tanaka A., Tobinaga S., *ibid.*, **40**, 3062—3066 (1992).
3) Kobayashi S., Sameshima. K., Ishii Y., Tanaka A., *Chem. Pharm. Bull.*, **43**, 1780—1790 (1995).
4) *a*) Poland A., Kuntson J. C., *Ann. Rev. Pharmacol. Toxicol.*, **22**, 517—554 (1982); *b*) Safe S. H., *ibid.*, **26**, 371—399 (1986).
5) *a*) Koga H., *Kagaku No Ryoiki, Zokan*, **136**, 177—202 (1982); *b*) Mitsuhashi S., "New quinolones," Gakkaisyuppan Center, Tokyo, Japan, 1991.
6) *a*) Parr R. G., Peason R. G., *J. Am. Chem. Soc.*, **105**, 7512—7516 (1983); *b*) Shankar S., Parr R. G., *Proc. Natl. Acad. Sci. U.S.A.*, **82**, 264—266 (1985); *c*) Pearson R. G., *Acc. Chem. Res.*, **26**, 250—255 (1993).
7) SPARTAN software, A general molecular orbital and mechanics package,ver.4.0, Wavefunction. Inc., U.S.A.
8) Parr R. G., Donnelly R. A., Palke W. E., *J. Chem. Phys.*, **68**, 3801—3807 (1978).
9) *a*) Staudenbauer W. L., Orr E., *Nucleic Acids Res.*, **9**, 3589—3603 (1981); *b*) Shen L. L., Kohlbrenner W. E., Weigl D., Baranowski J., *J. Biol. Chem.*, **264**, 2973—2978 (1989).
10) Ma Q., Dong L., Whitlock J. P., Jr., *J. Biol. Chem.*, **270**, 12697—12703 (1995).
11) Burbach K. M., Poland A., Bradfield C. A., *Proc. Natl. Acad. Sci. U.S.A.*, **89**, 8185—8189 (1992).
12) *a*) Matsumoto J., Miyamoto T., Minamida A., Nishimura Y., Egawa H., Nishimura H., *J. Med. Chem.*, **27**, 292—301 (1984); *b*) Domagala J. M., Hanna L. D., Heifetz C. L., Hutt M. P., Mich T. F., Sanchez J. P., Solomon M., *ibid.*, **29**, 394—404 (1986).
13) Cozzarelli N. R., *Science*, **207**, 953—960 (1980).
14) Denomme M. A., Leece B., Li A., Towner R., Safe S., *Biochem. Pharmac.*, **35**, 277—282 (1986).
15) *a*) Goldstein J. A., McKinney J. D., Lucier G. W., Hickman P., Bergman H., Moore J. A., *Toxicol. Appl. Pharmacol.*, **36**, 81—92 (1976); *b*) Yoshimura H., Ozawa N., Saeki S., *Chem. Pharm. Bull.*, **26**, 1215—1221 (1978); *c*) Yoshimura H., Yoshihara S., Ozawa N., Miki M., *Ann. N.Y. Acad. Sci.*, **320**, 179—192 (1979).
16) Dynes J. J., Baudais F. L., Boyd R. K., *Can. J. Chem.*, **63**, 1292—1299 (1985).
17) Kobayashi S., Kitadai M., Sameshima K., Ishii Y., Tanaka A., *J. Mol. Struct.*, in press, (1998).
18) Yoshida H., Bogaki M., Nakamura M., Yamanaka L. M., Nakamura S., *Agents Chemother.*, **35**, 1647—1650 (1991).
19) *a*) Phillips W. E. J., *Can. J. Biochem. Physio.*, **41**, 1793—1802 (1963); *b*) Robison A. K., Schemidt W. A., Stancel G. M., *J. Tox. Envir. Hlth.*, **16**, 493—508 (1985); *c*) Kelce W. R., Stone C. R., Laws S. C., Gray L. E., Kemppainen J. A., Wilson E. M., *Nature* (London), **375**, 581—585 (1995).
20) Sameshima K., Kobayashi S.; A part of this work was presented at 1997 Symposium on Computational and Theoretical Chemistry, June 23—24, 1997, Tokyo, Japan.